Journal of Magnetic Resonance 199 (2009) 68–74

Contents lists available at ScienceDirect

Journal of Magnetic Resonance

journal homepage: www.elsevier.com/locate/jmr

Water molecule contributions to proton spin–lattice relaxation in rotationally immobilized proteins

Yanina A. Goddard [a], Jean-Pierre Korb [b], Robert G. Bryant [a,*]

[a] Chemistry Department, University of Virginia, P.O. Box 400319, Charlottesville, VA 22904-4319, USA
[b] Laboratoire de Physique de la Matière Condensée, Ecole Polytechnique, CNRS, 91128 Palaiseau, France

ARTICLE INFO

Article history:
Received 7 January 2009
Revised 1 April 2009
Available online 8 April 2009

Keyword:
Spin–lattice relaxation, Magnetic relaxation dispersion
Water dynamics
Solid proteins
Field dependence

ABSTRACT

Spin–lattice relaxation rates of protein and water protons in dry and hydrated immobilized bovine serum albumin were measured in the range of ^{1}H Larmor frequency from 10 kHz to 30 MHz at temperatures from 154 to 302 K. The water proton spin–lattice relaxation reports on that of protein protons, which causes the characteristic power law dependence on the magnetic field strength. Isotope substitution of deuterium for hydrogen in water and studies at different temperatures expose three classes of water molecule dynamics that contribute to the spin–lattice relaxation dispersion profile. At 185 K, a water ^{1}H relaxation contribution derives from reorientation of protein-bound molecules that are dynamically uncoupled from the protein backbone and is characterized by a Lorentzian function. Bound-water-molecule motions that can be dynamically uncoupled or coupled to the protein fluctuations make dominant contributions at higher temperatures as well. Surface water translational diffusion that is magnetically two-dimensional makes relaxation contributions at frequencies above 10 MHz. It is shown using isotope substitution that the exponent of the power law of the water signal in hydrated immobilized protein systems is the same as that for protons in lyophilized proteins over four orders of magnitude in the Larmor frequency, which implies that changes in the protein structure associated with hydration do not affect the ^{1}H spin relaxation.

1. Introduction

The motions of water in or on biological macromolecules are of fundamental importance because the dynamics modulate intra- and inter-molecular energetics as well as macromolecular structure [1–4]. Although enormous progress has been made in characterizing the dynamics of water–protein systems, understanding remains incomplete. Nuclear magnetic relaxation dispersion (MRD), the measurement of nuclear spin–lattice relaxation-rate constants as a function of magnetic field strength, offers valuable information on molecular dynamics and structure. Nuclear spin relaxation is not spontaneous, but derives from coupling of the nuclear spins to the magnetic noise in the system, which in turn arises from molecular motion. The magnetic field dependence of the spin–lattice relaxation rate, i.e., the ^{1}H MRD profile, then provides a quantitative statistical characterization of the molecular dynamics that drive the spin relaxation; usually this is a map of the frequency dependence for the intra- and inter-molecular magnetic dipolar couplings.

Previous MRD studies of dry proteins have shown that the relaxation is described by a power law in the Larmor frequency, $\frac{1}{T_1} = A\omega^{-b}$, where A and b are constants [5–10]. The physical origin of the power law has been related to a spin–fracton relaxation mechanism [6,11–15]. The essential dynamical picture behind this relaxation mechanism is similar to those employed in vibrational network models for protein dynamics [16–18]. The propagation of structural fluctuations in the protein which modulate ^{1}H dipolar couplings that drive spin relaxation are characterized by a reduced dimensionality because of the limited or non-uniform connectivity in the folded protein structure [6,7,19]. The exponent, b, in the power law is related by the relaxation theory to a spectral dimension, d_s, which characterizes the vibrational density of states and the dimensionality of the disturbance propagation, and a fractal dimension, d_f, which describes the distribution of mass in space [6]. For dry proteins $b = 0.76 \pm 0.04$ [5,6,10,15,20,21]. In the rotationally immobilized systems, spin–spin couplings are efficient and a common spin temperature is established rapidly. As a consequence, motions that relax one group efficiently relax the whole ^{1}H spin population, which is observed as a single broad resonance line. Recent MRD studies of dry proteins and polypeptides over wide temperature ranges revealed the nature of the side-chain contributions to the ^{1}H spin relaxation [21,22]. At high and low frequencies, the field dependence is a power law because the main-chain fluctuations also modulate the side-chain couplings. A displacement of the high and low frequency power laws is

* Corresponding author. Fax: +1 434 924 3567.
E-mail address: rgb4g@virginia.edu (R.G. Bryant).

1090-7807/$ - see front matter © 2009 Elsevier Inc. All rights reserved.
doi:10.1016/j.jmr.2009.04.001

caused by the side-chain motions, which create a transition when the side-chain frequency approximates the proton Larmor frequency. The effects of the side-chain dynamics move into the experimental frequency range only at low temperatures using currently convenient magnetic fields [21,22]. The present experiments focus on relaxation contributions of protein-bound water dynamics, which in some cases look like a side-chain contribution in that the water motions may be coupled to the backbone dynamics. For other water molecules, the local motions are uncoupled from the backbone dynamics, which makes a relaxation contribution that may be distinguished from the coupled case based on the shape of the MRD profile.

Fig. 1 illustrates magnetic relaxation dispersion profiles for dry and hydrated bovine serum albumin at 302 K. The hydrated protein system is a valuable model of a more complex counterpart such as a tissue where the physical and chemical diversity of the components make detailed analysis problematic. A distinct and critical feature of the water ^{1}H relaxation dispersion profile of the heterogeneous water–protein system (Fig. 1) is that, analogous to the dry protein system, it is described by a power law in magnetic field strength or ^{1}H Larmor frequency. The efficient magnetization transfer or cross relaxation between protein and water–proton spins is responsible for this effect and has been widely studied [2,8,23–26]. The cross relaxation affects the response of both the water- and protein-spin populations. The usual model presumes that there are relatively few water molecules that are bound to the protein for times of hundreds of nanoseconds to several microseconds and is supported by solution phase MRD measurements that count the number of such molecules [27]. These unique molecules affect the relaxation rate of the whole water population through protein–water-proton and water–water-proton dipolar interactions coupled with proton and water molecule exchange from bound to bulk environments. In earlier work, the changes in the MRD profile on hydration were attributed to changes in the power law exponent given by $b = 3 - 2\frac{d_S}{d_f} - d_S$ [6,15]. The change in b was ascribed to structural changes in the protein upon hydration that affected the special distribution of protons, and therefore, d_f [6]. In this paper we reexamine this intriguing issue and show that the water content dependence of the power law exponent is not supported by more complete data sets that span a larger range of temperature and frequency. Further, studies at low temperature reveal bound-water-molecule motions that are independent of the protein-backbone fluctuations and characterized by a Lorentzian relaxation dispersion profile.

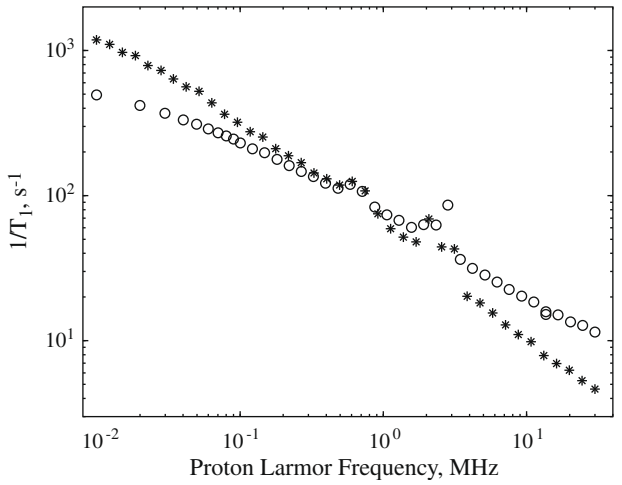

Fig. 1. The proton spin–lattice relaxation-rate constants as a function of magnetic field strength plotted as the proton Larmor frequency for dry (stars) and hydrated to 0.32 g H_2O/g protein (open circles) bovine serum albumin at 302 K. The peaks in the relaxation profiles of all samples between 0.5 and 5 MHz are due to ^{14}N–^{1}H level crossing [45].

2. Experimental

Bovine serum albumin (BSA) obtained from Sigma Chemical Company (St. Louis, MO) was dialyzed against at least five changes of deionized water. The protein was lyophilized using a mechanical vacuum at 298 K. Solvated samples were prepared by adding the desired mass of solvent, such as deionized water or deuterium oxide (99.9 atom % D, Cambridge Isotope Laboratories, Inc., Andover, MA) to a known mass of protein. Hydrated protein samples were allowed to equilibrate for at least 3 days at 310 K. The amount of moisture in hydrated BSA samples was additionally checked by a Karl Fischer titrator (Aquatest 8, Photovolt Instruments, Inc., Indianapolis, IN). The hydrated protein samples used in this study were prepared to contain 0.32 g water per 1.0 g of protein. It has been shown that as the level of hydration of small globular proteins increases above 0.38 g water/g protein, the protein can be considered fully hydrated in a sense that further addition of water does not change its spectroscopic or thermodynamic properties as compared to fully hydrated (1.0 g water/0.1 g protein) protein gels [3,4,28–30]. Since, to first approximation, the number of water molecules in direct contact with the protein at any given time is proportional to the surface area of the protein, which correlates with molecular weight, the larger proteins are believed to be fully hydrated at slightly lower water levels [31].

For BSA samples prepared with D_2O, 1.0 g of BSA was initially dissolved in 20 mL of D_2O and stirred at 325 K for 4 h, then transferred to a Centricon filter (Millipore; 30,000 MW cut-off) and concentrated to 5 mL in the centrifuge. The concentrated solution was diluted again to 20 mL with D_2O as the procedure was repeated 4 times to minimize the number of exchangeable protons remaining on the protein. Finally, the protein was lyophilized at 337.8 K using a drying pistol with refluxing methanol and a mechanical vacuum.

The nuclear magnetic resonance data were recorded using an FFC-2000 fast field cycling NMR spectrometer (Stelar s.r.l., Mede, Italy). The Stelar spectrometer provides temporal control of the magnetic field; in the present experiments the field-switching time used was 3 ms. Proton spins were polarized at 30 MHz and free induction decays were recorded following a single (6.7 μs) 90° excitation pulse applied at 15.8 MHz [32]. The relaxation fields were varied between ^{1}H Larmor frequency 0.01 and 30 MHz. The spectrometer dead time was 11 μs. The NMR signal was averaged (at least 8 scans) for at most 32 linearly spaced time sets, each of which was adjusted at every relaxation field to optimize the sampling of the decay/recovery curves. Within experimental error, all the decay/recovery curves of longitudinal magnetization were exponential. Temperature was varied from 154 K to 302 K using a Stelar VTC90 variable temperature controller, which was calibrated using an external thermocouple inserted into a surrogate sample at the resonance position in the probe. Based on repeated calibrations, the temperature in all NMR experiments was controlled to within 0.5 K. Samples were allowed to equilibrate for at least 20 min at each temperature before data acquisition.

3. Results and discussion

The proton transverse magnetization decay of dry protein can be described well by a single Gaussian with a decay time on the order of 10 μs, but for hydrated protein powders the transverse magnetization decay is multi-component [33]. The rapid transverse decay is characteristic of solid protein. The slow transverse decay includes contributions from water- and protein-side-chain protons

which are sufficiently mobile that the dipolar couplings are at least partially averaged by motion. When the temperature of the hydrated protein sample is reduced, the fraction of slowly decaying or "liquid" components of the *xy*-magnetization decreases until the sample crosses the so-called glass transition temperature [33–39] below which all observed protons become magnetically equivalent and only a single rapid transverse magnetization decay is observed. Previous study has shown that water in a hydrated sample of BSA forms what is magnetically a solid around the protein at approximately 170 K [33].

Fig. 2 compares the relaxation dispersion profile of dry BSA to that of hydrated BSA at 154 K where water protons were replaced by deuterons. The hydrated sample was prepared using BSA in which labile protons were exchanged for deuterons to minimize the effect of liquid-phase protons. This preparation allows observation of all non-exchangeable protein protons when the system is hydrated with D_2O. Within experimental error, the data sets overlap. As can be seen from Fig. 2, the magnetic relaxation dispersions at low temperature differ from that observed at 302 K [22]. The difference is in the high field portion of the relaxation dispersion profile, which at low temperatures, preserving the power law, is displaced to higher relaxation rates relative to the extrapolation of the low field profile. This phenomenon was previously described in [21,22], where it is shown that the increase in the relaxation rates is due to fast motion of covalently bound protein-side-chain groups. Motion of phenyl rings was observed at low frequencies and elevated temperatures for polyphenylalanine while motions of methyl groups dominate at high frequency and low temperatures [22]. Even though the motion of side-chain methyl groups is present at all temperatures, it is sufficiently slow only below 180 K for dry BSA to enter the observation window and offset the relaxation-rate constant to larger values at the highest frequencies as shown in Fig. 2 for BSA at 154 K; nevertheless, the power law in the Larmor frequency is preserved [21,22]. The dashed in Fig. 2 was simulated using Eq. (1) that summarizes the spin–fracton relaxation mechanism for rotationally immobilized protein protons [6]

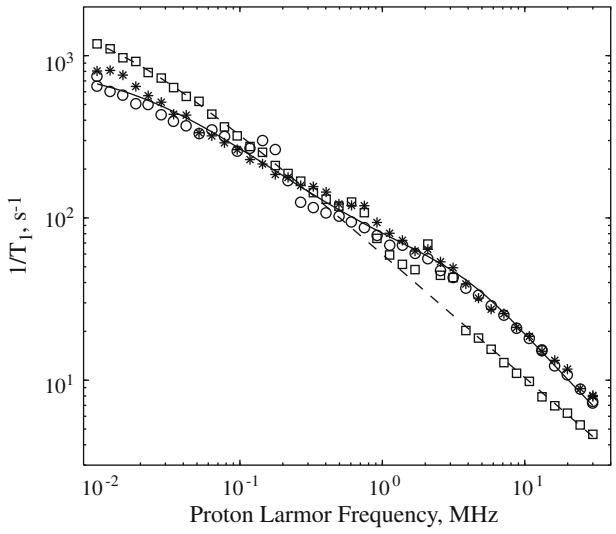

Fig. 2. The proton spin–lattice relaxation-rate constants as a function of magnetic field strength plotted as the proton Larmor frequency for dry bovine serum albumin at 154 K (stars) and 302 (squares) as well as for deuterated bovine serum albumin hydrated to 0.32 g ^2H_2O/g protein (circles) at 154 K. The dashed line is the best fit to Eq. (1) with $b = 0.76$, $M_2 = 7.98 \times 10^9\ s^{-2}$ and dipolar coupling strength $\omega_D = 0.01$ MHz. The solid line is the best fit to Eq. (2) obtained with the parameters: $b = 0.78$; correlation time for methyl-group jumps, $\tau_{CH3} = 35$ ns; and $C\frac{N_{CH_3}}{N_H} = 8$ (see Ref. [21]). The second moment, $M_2 = 1.01 \times 10^{10}\ s^{-2}$, was measured as described in [33] and the dipolar coupling strength was calculated as $\omega_D = \sqrt{\frac{20M_2}{9}}$.

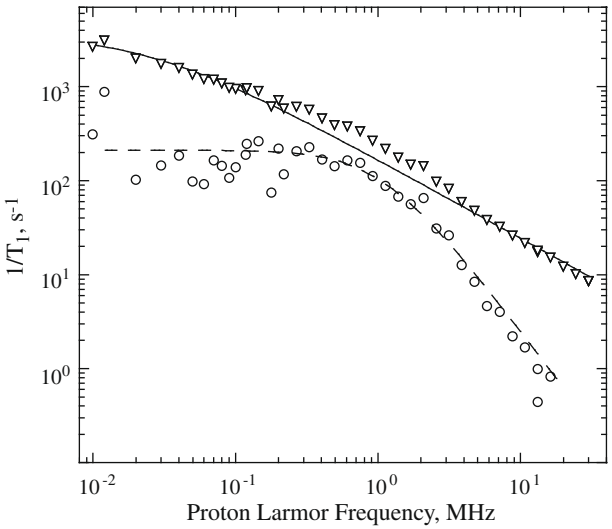

Fig. 3. The proton spin–lattice relaxation-rate constants as a function of magnetic field strength plotted as the proton Larmor frequency for bovine serum albumin hydrated to 0.32 g H_2O/g protein at 185 K (triangles). The solid line is the best fit to Eq. (1) with $b = 0.84$. The second moment, $M_2 = 1.14 \times 10^{10}\ s^{-2}$, was measured as described in [33] and the dipolar coupling strength was calculated as $\omega_D = \sqrt{\frac{20M_2}{9}}$. The difference between experimental data points and the fit are depicted as open circles. The dashed line is the best fit to $\frac{1}{T_1} = B(J(\omega) + 4J(2\omega))$, where the reduced spectral density $J(\omega)$ is a Lorentzian function with correlation time for stochastic jumps $\tau_c = 92$ ns. B is the scaled dipolar coupling strength of the intra-molecular interaction of water protons that are separated by 1.58 Å and was found to equal $4.57 \times 10^8\ s^{-2}$, which implies that the scaling factor, $\frac{N_{H2O}}{N_{Total}}$, equals to 4.2×10^{-2}. Here N_{H2O} is the number of non-frozen water protons and N_{Total} is the total number of protons in the system. Within experimental error, the scaling factor is consistent with the fraction of liquid component of the transverse magnetization decay at 185 K (5% of total magnetization [33]).

and employing the non-linear Levenburg–Marquardt least-squares procedure:

$$\frac{1}{T_{1D\text{-}chain}} = 3\pi k_B T d_S \frac{\bar{M}_2}{\hbar} \Omega_{//}^{b-2} \left(1 + \frac{1}{2^b}\right) \omega^{-b}. \tag{1}$$

Here $\omega = \omega_0 + \omega_D$, ω_0 is the precession frequency associated with the applied magnetic field, ω_D is the frequency associated with the local proton dipolar field, T is the absolute temperature, k_B is Boltzmann constant, $\bar{M}_2$ is the proton second moment that characterizes the strength of the dipolar coupling and is measured directly from the time decay of the free precession signal [33], and $\hbar\Omega_{//}$ is the energy for the vibrational transition parallel with the polypeptide backbone that is approximated by the amide (II) transitions. The parameters obtained from this fit are listed in the figure legend. The solid line in Fig. 2 is a best fit to Eq. (2), which assumes a strong dynamical coupling of the protein-side-chain groups and protein-backbone motions [21]:

$$\frac{1}{T_1} = \frac{1}{T_{1D\text{-}chain}} + 3\pi k_B T d_S \tau_f^b(T) \bar{M}_2 C \frac{N_{CH_3}}{N_H} \times \frac{\Omega_{//}^{b-2}}{\hbar} \left(1 + \frac{1}{2^b}\right) \frac{\cos[b \arctan(\omega\tau_{CH_3}(T))]}{\cos(b\frac{\pi}{2})(1 + \omega^2\tau_{CH_3}^2(T))^{b/2}}, \tag{2}$$

where N_{CH_3} is the number of rapidly moving proton spins in a protein, N_H is number of rigid protein protons, C is a numerical constant that arises due to the structural and dynamical differences of the protons that surround the reference spin, τ_{CH_3} is a correlation time for the motion of side-chain groups. It is interesting to note that the hydration glass formed by D_2O affects the ^1H spin relaxation very little even though the side-chain orientations are different in the dry compared to the hydrated protein [33].

At 185 K a small ^{1}H transverse component (~5% of total magnetization) demonstrates that some protons are sufficiently mobile that local dipole–dipole coupling is partially averaged by motion. Fig. 3 illustrates spin–lattice relaxation-rate constants for a hydrated BSA sample as a function of proton Larmor frequency obtained by observing the rapidly decaying transverse magnetization at 185 K. The solid line in Fig. 3 was calculated as the best fit using a Levenburg–Marquardt algorithm applied to Eq. (1). There is a small but significant disagreement between the fit and the data in the range 0.2–7 MHz at 185 K that is most apparent when the fitted curve is subtracted from the experimental data. The difference is shown in Fig. 3 and fitted to a Lorentzian function (dashed line) with a correlation time of 92 ns. The Lorentzian shape is expected when relaxation is dominated by the rotationally correlated dipolar coupling [40]. At this temperature the frequency of side-chain group motions is just above the observation frequency window; in addition, these coupled side-chain motions do not create a Lorentzian MRD contribution [21]. If water- and protein-proton motions are independent and dynamically uncoupled, the relaxation equation may be written as a sum of terms, one from the backbone dynamics and one from the water reorientation described by a Lorentzian function. This approach describes the magnetic field dependence of the longitudinal relaxation-rate constant shown in Fig. 3. This case is distinct from that where water molecules form one or more long-lived hydrogen bonds with the protein that may couple the water spins for time long enough to sense the characteristics of the protein-backbone fluctuations. In the dynamically coupled case, the water relaxation would make a contribution similar to that of methyl side-chain groups [21,22]. Because the Lorentzian function adequately describes the excess relaxation contribution in Fig. 3, we identify it with non-frozen water molecules that are situated within the regions where they interact most weakly with the protein, such as hydrophobic pockets where there is no strong hydrogen bond to tie the water reorientation to the protein fluctuations. If these molecules were dynamically coupled to the backbone, the Lorentzian fit would fail.

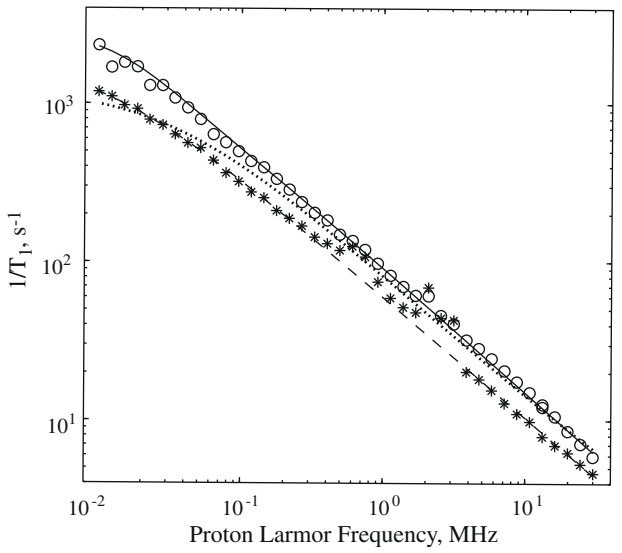

Fig. 4. The proton spin–lattice relaxation-rate constants as a function of magnetic field strength plotted as the proton Larmor frequency for dry bovine serum albumin at 302 K (stars) and bovine serum albumin hydrated to 0.32 g H_2O/g protein at 154 K (open circles). The dashed line is the best fit to Eq. (1) with $b = 0.76$ and dipolar coupling strength $\omega_D = 0.01$ MHz. The second moment, $M_2 = 7.98 \times 10^9$ s^{-2}, was measured as described in [33]. The solid line is the best fit to a sum of the solid protein-backbone relaxation contribution summarized in Eq. (1) with $b = 0.783$ and the contribution of the stochastic motion of water $B(J(\omega) + 4J(\omega))$, where $J(\omega)$ is a Lorentzian function. The second moment for the hydrated sample was $M_2 = 1.74 \times 10^{10}$ s^{-2} [33] and the dipolar coupling strength was calculated as $\omega_D = \sqrt{\frac{20M_2}{9}}$. The dotted line illustrates the solid protein contribution (Eq. (1)) without the Lorentzian term for BSA/H_2O sample at 154 K.

Hydration of the protein to the same level with ^1H_2O instead of ^2H_2O changes the MRD profile at 154 K in two significant ways as shown in Fig. 4. First, the ^{1}H relaxation-rate constants are higher for the BSA/H_2O sample; at 10 kHz the rate exceeds 2000 s^{-1}. The MRD profile of dry BSA at 302 K is shown in Fig. 4 for comparison. Not only are the relaxation rates for the hydrated sample collected at the lower temperature larger, but also the two MRD profiles are not parallel. Second, in the log–log presentation, the relaxation profile of the H_2O sample is a straight line and the offset to higher rates induced by methyl rotational jumps is not resolved. These differences derive from the dynamics and magnetic coupling of the water protons to the protein spin system.

Eqs. (1) and (2) show that the relaxation-rate constant is a linear function of temperature. Between 154 and 302 K the relaxation rate should increase by a factor of 2, but hydration disrupts this temperature dependence. At 154 K, which is below the "glass" transition, a single rapid transverse magnetization decay is observed [33]. At this temperature all water protons are immobilized effectively filling surface irregularities created by the protein secondary and tertiary structures, thus adding water-proton spins that are magnetically indistinguishable from protein-proton spins to the sum in the ^{1}H second moment [40]. This increased number of solid protons increases the ^{1}H second moment of the hydrated sample approximately 5-fold from room temperature to 154 K [33]. Because the relaxation rate is directly proportional to the second moment as shown by Eqs. (1) and (2), the change in the second moment dominates the effects of the temperature change and the relaxation rate increases.

There is no evidence that hydration should stop methyl-group reorientation or eliminate this contribution to relaxation; nevertheless, a methyl offset is not apparent in Fig. 4. For this BSA/H_2O sample, the total rigid proton-spin population, N_H, is much larger below the "glass" transition temperature than that of dry or BSA/D_2O samples and includes the water protons as well as the protein protons. Since the magnitude of the methyl-proton relaxation contribution is proportional to the population fraction $\frac{N_{CH_3}}{N_H}$ and the number of methyl groups, N_{CH3}, is independent of hydration while the total number of protons, N_H, increases substantially with hydration, the methyl groups are less efficient in the relaxing whole solid proton population of the BSA/H_2O system at low temperatures. BSA has approximately 4400 protons, 939 of which are methyl protons. At the hydration level of 0.32 g BSA per 1 g of water, around 2500 of H_2O protons are added to the system. This translates into more than 70% increase of rigid proton population as temperature is lowered below the glass transition. Thus, the increase in the relaxation rates due to methyl dynamics is less pronounced and on the order of the uncertainty. Indeed, Shirley and Bryant [41] observed that, at 57.5 MHz, water protons constitute a relaxation sink for the protein protons in a hydrated lysozyme sample at high temperatures, while at low temperature the water protons add to the relaxation load of the methyl protons and the relaxation is less efficient than that in the dry case.

The solid line in Fig. 4 is the best fit to the relaxation equation that consists of two contributions: one from the protein dynamics described by Eq. (1) and a Lorentzian term attributed to stochastic rotational jumps of non-bonded water identified in the discussion of Fig. 3. Because the lowest relaxation frequency was 10 kHz and the rates at low frequencies for this sample were quite high, it was not possible to sample the Lorentzian contribution completely enough to define the correlation time uniquely. The dotted line in Fig. 4 shows just the term for protein-backbone dynamics, neglecting the Lorentzian contribution and clearly falls below the data at low field strengths. This curve also illustrates that an increase in

the proton second moment at 154 K translates to an increase in local proton dipolar coupling and a more pronounced low field plateau. The solid line includes the Lorentzian contribution with a correlation time of 5 μs; this value is larger than that at 185 K as expected but it is quite uncertain as noted above. Nevertheless, the exponent of the power law, b, is equal to 0.78 ± 0.04 and independent of the correlation time for the Lorentzian function.

It is well known that coupling of "liquid" and "solid" populations in hydrated protein systems results in bi-exponential decay of the longitudinal magnetization described by solutions of a system of two coupled differential equations [8,23,42]. In principle, the roots of the coupled equations may be detected by observing either the protein- or the water-spin population. In the present study, a short 90° pulse was applied to the whole spin system so that initial reduced magnetizations of water protons and protein protons were equal. With these initial conditions, and in the limiting case where the rate of magnetization transfer between two populations is much larger than water- or protein-proton relaxation rates, that is, in the limit of efficient coupling, one of the pre-exponential coefficients of the solution of the differential equation system for both liquid and solid components becomes small, so that the longitudinal magnetization for these components has a single exponential character and the relaxation-rate constants may be extracted from either magnetization. This situation obtains generally at high field strengths. In the opposite limit, where the protein-proton relaxation-rate constant is much larger than the water-proton relaxation rate and magnetization transfer rate, i.e., at very low frequencies, z-magnetization of water protons again exhibits a mono-exponential character because one pre-exponential factor is small and the observed rate is limited by the magnetization transfer rate. At the same time the bi-exponential character of the solid-protein-proton magnetization is preserved, which makes analysis of the protein-proton decay a subject to the difficulties of multi-exponential analysis.

Water and protein relaxation-rate constants can be measured separately by exploiting differences in the transverse decay rates of these components. In the present study, the water relaxation-rate constant was determined by analyzing the transverse magnetization as a function of the relaxation field evolution time with 66 μs acquisition delay following the 90° sampling pulse at the resonance field. The solid-protein relaxation rate was found by subtracting the fit of the water transverse magnetization obtained at long times from the total transverse magnetization during the first 12 μs of the free induction decay and then analyzing the difference as a function of time in the relaxation field. The details of the transverse magnetization fit procedures have been described previously [33]. Fig. 5 illustrates protein and water relaxation-rate constants at 302 K and it is clear that there are systematic differences between the liquid and solid component analysis at low fields. This difference is critical to understand because it suggests an apparent failure of the coupled relaxation model that accounts for so much data well. The elevated values for the solid component rate constants at low fields are caused by the difficulty of separating the fast and slow components of the longitudinal magnetization decay as noted above for the protein. Therefore, these values are more subject to a systematic error associated with sums of exponentials than the water proton decays. Thus, only the water component was analyzed in the present work. The solid line in Fig. 5 is the best fit to the equation [26]:

$$\frac{1}{T_1}=\frac{1}{2}\left(\frac{1}{T_W}+\frac{1}{T_P}+\frac{1}{T_{WP}}\left(1+\frac{1}{F}\right)-\left(\left(\frac{1}{T_P}-\frac{1}{T_W}-\frac{1}{T_{WP}}\left(1-\frac{1}{F}\right)\right)^2+\frac{4}{FT_{WP}^2}\right)^{1/2}\right) \tag{3}$$

where $\frac{1}{T_{WP}}$ is the magnetization transfer rate, F is the ratio of the equilibrium transverse magnetization of protein protons to that of water protons, $\frac{1}{T_P}$ is the protein-proton relaxation rate, described by spin–fracton theory (Eq. (1)) with exponent $b = 0.783$ and $\frac{1}{T_W}$ is the relaxation rate for water. The relaxation-rate constant $\frac{1}{T_W}$ is usually assumed to be field independent, but there are several contributions that are important at high field strengths.

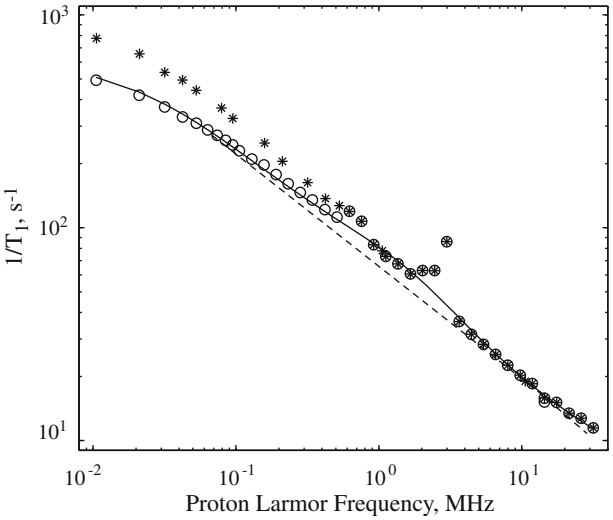

Fig. 5. The proton spin–lattice relaxation-rate constants as a function of magnetic field strength plotted as the proton Larmor frequency for fast (stars) and slowly (open circles) decaying portion of the free induction decay of bovine serum albumin hydrated to 0.32 g H_2O/g protein at 302 K. The solid line is the best fit to the Eq. (3) with the protein relaxation contribution summarized in Eq. (1) with $b = 0.79$ and the water contribution that consists of three terms as described in the text. The correlation time for surface diffusion was fixed at 15 ps. The second moment, $M_2 = 4.56 \times 10^9\ s^{-2}$, was measured as described in [33] and the dipolar coupling strength was calculated as $\omega_D = \sqrt{\frac{20M_2}{9}}$. The additional parameters of this fit were the magnetization transfer rate, the constant factors of water surface diffusion and water rotational jumps, and the correlation time for water rotational jumps. For the model of heterogeneous water–protein system, fits that include five variable parameters are not unique. However, the precise value of four not listed parameters do not impact the discussion presented in this manuscript. The correlation time for water rotational jumps was model dependent as discussed in text and found to be 50 ± 30 ns. The dashed power-law line is drawn to guide the eye.

The first water contribution is from the bulk water relaxation, which is a constant equal to 0.28 s^{-1} for pure water at 298 K. When oxygenated in air, this rate constant increases to approximately 0.33 s^{-1} but becomes field dependent because of the translational motion of water near the paramagnetic oxygen and the electron spin–lattice relaxation [43]. The low field dispersion is at a proton Larmor frequency of approximately 33 MHz, while the high field dispersion is at approximately 22 GHz and beyond the range of presently practical magnetic fields. The second contribution derives from the translational exploration of the protein surface by water that is practically two-dimensional because of the geometrical constraints of the surface. It has been shown for protein solutions that this motion can be described by a logarithmic field dependence of the relaxation-rate constant with an average correlation time of 15 ± 3 ps for the water–water intermolecular contribution [44]. The third contribution derives from fast stochastic rotational jumps of water molecules that experience long-lived interactions with the protein. These unique water molecules may be bound to the protein with hydrogen bond(s), leading to the power law in the Larmor frequency, or they can be located in hydrophobic crevasses on the protein with no dynamical coupling to the backbone, as noted earlier for the data in Fig. 3. The solid line shown in Fig. 5 was computed neglecting the oxygen field dependence and the Lorentzian contribution from the dynamically uncoupled water molecules but including the logarithmic term associated with surface water diffusion and the

dynamically coupled model represented by Eq. (2) for the protein-bound water contribution [21]. We note that if the bound water is modeled as a Lorentzian the fit is comparable. Although the data at lower temperature resolves contributions from dynamically uncoupled water molecules and it seems likely that both coupled and uncoupled contributions are present at room temperature, only one of these contributions was required to simulate the experimental data set within experimental error. Some distribution of local dynamics of the coordinated water molecules seems probable because there is a considerable distribution of structure likely at different interaction sites; however, a single correlation time provides an adequate fit for the experimental data set, as shown in Fig. 5. The correlation time for the rotational stochastic jumps of the bound water molecules were model dependent and on average around 50 ± 30 ns. The dashed power-law line in Fig. 5 is drawn to guide the eye. It illustrates the low field plateau, which is predominantly due to magnetization transfer effects for this sample at this temperature, the "bump" from the rotational motion of bound water molecules at intermediate frequencies and the high-frequency tail from water translational diffusion. It is important to emphasize that the exponent of the power law of the water signal was found to be 0.78 ± 0.06 whether jumps due to non-hydrogen-bonded or hydrogen-bonded water proton contribution were considered in the fit. This value for the hydrated case is the same as that for the lyophilized protein. Consequently, since b is associated with the spectral and fractal dimensions, this result implies a small change, if any, in the protein structure upon the hydration.

4. Conclusions

Measurements of the relaxation dispersion profiles of hydrated immobilized protein systems at different temperatures reveal several different classes of molecular dynamics that affect ^{1}H spin–lattice relaxation. An efficient magnetization transfer within a water-immobilized protein system leads to the characteristic power law in the Larmor frequency of the water-proton MRD profile. The relaxation-rate constants of the water signal are limited by the magnetization transfer rate at low frequencies (10–300 kHz), resulting in lower values of the spin–lattice decay constants compared to those of dry protein systems. At higher Larmor frequencies, the contributions that derive from translational diffusion of water near the protein surface as well as stochastic rotational motion of long-lived coordinated water protons cause an increase in the ^{1}H relaxation rates compared to the dry sample. Combining these water-proton contributions with the spin–fracton relaxation mechanism of the protein provides a satisfactory description of the magnetic relaxation behavior of water proton spins in heterogeneous protein systems. The present experiments demonstrate that the power law exponent, b, does not change with protein hydration.

Acknowledgment

This work was supported by the National Institutes of Health, RO1 NIBIB 2805, the University of Virginia, the CNRS and Ecole Polytechnique, France.

References

[1] B. Bagchi, Water dynamics in the hydration layer around proteins and micelles, Chem. Rev. 105 (2005) 3197–3219.
[2] R.G. Bryant, The dynamics of water–protein interactions, Annu. Rev. Biophys. Biomol. Struct. 25 (1996) 29–53.
[3] I.D. Kuntz, W. Kauzmann, Hydration of proteins and polypeptides, Adv. Protein Chem. 28 (1974) 239–345.
[4] J.A. Rupley, P.-H. Yang, G. Tollin, Thermodynamic and related studies of water interacting with proteins, in: S.P. Rowland (Ed.), Water in Polymers, American Chemical Society, Washington, DC, USA, 1980, pp. 111–132.
[5] R. Kimmich, E. Anoardo, Field-cycling nmr relaxometry, Prog. Nucl. Magn. Reson. Spectrosc. 44 (2004) 257–320.
[6] J.P. Korb, R.G. Bryant, The physical basis for the magnetic field dependence of proton spin–lattice relaxation rates in proteins, J. Chem. Phys. 115 (2001) 10964–10974.
[7] J.P. Korb, A. Van-Quynh, R.G. Bryant, Low-frequency localized spin-dynamical coupling in proteins, C. R. Acad. Sci. II C 4 (2001) 833–837.
[8] C.C. Lester, R.G. Bryant, Water-proton nuclear magnetic relaxation in heterogeneous systems: hydrated lysozyme results, Magn. Reson. Med. 22 (1991) 143–153.
[9] F. Noack, Nmr field-cycling spectroscopy: principles and applications, Prog. Nucl. Magn. Reson. Spectrosc. 18 (1986) 171–276.
[10] W. Nusser, R. Kimmich, Protein backbone fluctuations and NMR field-cycling relaxation spectroscopy, J. Phys. Chem. 94 (1990) 5637–5639.
[11] S. Alexander, Vibrations of fractals and scattering of light from aerogels, Phys. Rev. B 40 (1989) 7953–7965.
[12] S. Alexander, R. Orbach, Density of states on fractals: fractons, J. Phys. Lett. 43 (1982) L625–L631.
[13] R. Orbach, Dynamics of fractal networks, Science 231 (1986) 814–819.
[14] H.J. Stapleton, J.P. Allen, C.P. Flynn, D.G. Stinson, S.R. Kurtz, Fractal form of proteins, Phys. Rev. Lett. 45 (1980) 1456–1459.
[15] J.-P. Korb, R.G. Bryant, Noise and functional protein dynamics, Biophys. J. 89 (2005) 2685–2692.
[16] S. Reuveni, R. Granek, J. Klafter, Proteins: coexistence of stability and flexibility, Phys. Rev. Lett. 100 (2008) 208101–208104.
[17] I. Bahar, B. Erman, T. Haliloglu, R.L. Jernigan, Efficient characterization of collective motions and interresidue correlations in proteins by low-resolution simulations, Biochemistry 36 (1997) 13512–13523.
[18] P. Doruker, R.L. Jernigan, I. Bahar, Dynamics of large proteins through hierarchical levels of coarse-grained structures, J. Comput. Chem. 23 (2002) 119–127.
[19] J.P. Korb, A. Van-Quynh, R.G. Bryant, Proton spin relaxation induced by localized spin-dynamical coupling in proteins, Chem. Phys. Lett. 339 (2001) 77–82.
[20] W. Nusser, R. Kimmich, F. Winter, Solid state NMR study of protein polypeptide backbone fluctuations interpreted by multiple trapping of dilating defects, J. Phys. Chem. 92 (1988) 6806–6814.
[21] Y. Goddard, The magnetic field and temperature dependences of proton spin–lattice relaxation in proteins, J. Chem. Phys. 126 (2007) 175105.
[22] Y. Goddard, J.-P. Korb, R.G. Bryant, Nuclear magnetic relaxation dispersion study of the dynamics in solid homopolypeptides, Biopolymers 86 (2007) 148–154.
[23] H.T. Edzes, E.T. Samulski, The measurements of cross-relaxation effects in the proton NMR spin–lattice relaxation of water in biological systems: hydrated collagen and muscle, J. Magn. Reson. 31 (1978) 207–229.
[24] D.P. Hinton, R.G. Bryant, ^{1}H magnetic cross-relaxation between multiple solvent components and rotationally immobilized protein, Magn. Reson. Med. 35 (1996) 497–505.
[25] S.H. Koenig, R.D. Brown, A molecular theory of relaxation and magnetization transfer: application to cross-linked BSA, a model for tissue, Magn. Reson. Med. 30 (1993) 685–695.
[26] D. Zhou, R.G. Bryant, Magnetization transfer, cross-relaxation, and chemical exchange in rotationally immobilized protein gels, Magn. Reson. Med. 32 (1994) 725–732.
[27] A. Van-Quynh, S. Willson, R.G. Bryant, Protein reorientation and bound water molecules measured by ^{1}H magnetic spin–lattice relaxation, Biophys. J. 84 (2003) 558–563.
[28] F. Eisenhaber, P. Argos, Hydrophobic regions on protein surfaces: definition based on hydration shell structure and a quick method for their computation, Protein Eng. 9 (1996) 1121–1133.
[29] F. Franks, Solvation interactions of proteins in solution, Philos. Trans. R. Soc. Lond. B 278 (1977) 89–96.
[30] G. Diakova, Y. Goddard, J.-P. Korb, R.G. Bryant, Changes in protein structure and dynamics as a function of hydration from ^{1}H second moments, J. Magn. Reson. 189 (2007) 166–172.
[31] S. Miller, J. Janin, A.L. Lesk, C. Chothia, Interior and surface of monomeric proteins, J. Mol. Biol. 196 (1987) 641–656.
[32] G. Ferrante, S. Sykora, Technical aspects of fast field cycling, Adv. Inorg. Chem. 57 (2005) 405–470.
[33] Y. Goddard, J.-P. Korb, R.G. Bryant, Structural and dynamical examination of the low-temperature glass transition in serum albumin, Biophys. J. 91 (2006) 3841–3847.
[34] W. Doster, S. Cusack, W. Petry, Dynamical transition of myoglobin revealed by inelastic neutron scattering, Nature 337 (1989) 754–756.
[35] W. Doster, S. Cusack, W. Petry, Dynamic instability of liquidlike motions in a globular protein observed by inelastic neutron scattering, Phys. Rev. Lett. 65 (1990) 1080–1083.
[36] C. Baysal, A.R. Atilgan, Relaxation kinetics and the glassiness of proteins: the case of bovine pancreatic trypsin inhibitor, Biophys. J. 83 (2002) 699–705.
[37] C. Baysal, A.R. Atilgan, Relaxation kinetics and the glassiness of native proteins: coupling of timescales, Biophys. J. 88 (2005) 1570–1576.
[38] A.L. Tournier, J.C. Smith, Principal components of the protein dynamical transition, Phys. Rev. Lett. 91 (2003) 208106.

[39] D. Vitkup, D. Ringe, G.A. Petsko, M. Karplus, Solvent mobility and the protein 'glass' transition, Nat. Struct. Biol. 7 (2000) 34–38.
[40] A. Abragam, The Principles of Nuclear Magnetism, Oxford University Press, The Clarendon Press, Oxford, 1961.
[41] W.M. Shirley, R.G. Bryant, Proton-nuclear spin relaxation and molecular dynamics in the lysozyme–water system, J. Am. Chem. Soc. 104 (1982) 2910–2918.
[42] S.H. Koenig, R.G. Bryant, K. Hallenha, G.S. Jacob, Magnetic cross-relaxation among protons in protein solutions, Biochemistry 17 (1978) 4348–4358.
[43] C.-L. Teng, H. Hong, S. Kiihne, R.G. Bryant, Molecular oxygen spin–lattice relaxation in solutions measured by proton magnetic relaxation dispersion, J. Magn. Reson. 148 (2001) 31–34.
[44] Y.A. Goddard, G. Diakova, J.-P. Korb, R.G. Bryant, Dimensionality of water diffusive exploration at the protein interface in solution, J. Am. Chem. Soc., submitted for publication.
[45] R. Kimmich, W. Nusser, F. Winter, In vivo NMR field-cycling relaxation spectroscopy reveals $^{14}N^{1}H$ relaxation sinks in the backbones of proteins, Phys. Med. Biol. 29 (1984) 593–596.